Available online at www.sciencedirect.com
SCIENCE DIRECT®
Journal of Solid State Chemistry 174 (2003) 342–348
JOURNAL OF SOLID STATE CHEMISTRY
http://elsevier.com/locate/jssc

Sugar–anionic clay composite materials: intercalation of pentoses in layered double hydroxide

Sumio Aisawa, Hidetoshi Hirahara, Kayoko Ishiyama, Wataru Ogasawara, Yoshio Umetsu, and Eiichi Narita*

Department of Chemical Engineering, Faculty of Engineering, Iwate University, 4-3-5 Ueda, Morioka, Iwate 020-8551, Japan

Received 2 January 2003; received in revised form 16 April 2003; accepted 25 April 2003

Abstract

The intercalation of non-ionized guest pentoses (ribose and 2-deoxyribose) into the Mg–Al and Zn–Al layered double hydroxides (LDHs) was carried out at 298 K by the calcination–rehydration reaction using the Mg–Al and Zn–Al oxide precursors calcined at 773 K. The resulting solid products reconstructed the LDH structure with incorporating pentoses, and the maximum amount of ribose intercalated by the Mg–Al oxide precursor was approximately 20 times that by the Zn–Al oxide precursor. The ribose/Mg–Al LDH was observed to have the expanded LDH structure with a broad (003) spacing of 0.85 nm. As the thickness of the LDH hydroxide basal layer is 0.48 nm, the interlayer distance of the ribose/Mg–Al LDH is 0.37 nm. This value corresponds to molecular size of ribose in thickness (0.36 nm), supporting that ribose is horizontally oriented in the interlayer space of LDH. The maximum amount of ribose intercalated by the Mg–Al oxide precursor was approximately 5 times that of 2-deoxyribose. Ribose is substituted only by the hydroxyl group at C-2 position for 2-deoxyribose. Therefore, the number of hydroxyl group of sugar is essentially important for the intercalation of sugar molecule into the LDH, suggesting that the intercalation behavior of sugar for the LDH was greatly influenced by hydrogen bond between hydroxyl group of the intercalated pentose and the LDH hydroxide basal layers.

Keywords: Layered double hydroxides; Intercalation; Calcination–rehydration reaction; Sugar; Nanocomposite; Organic–inorganic hybrid materials

1. Introduction

Layered double hydroxides (LDHs), alternately known as anionic clays, and their intercalation compounds have received considerable attention in recent years in view of their potential technological importance as catalysis, electrode, optical memory, separator, adsorbent, and new nanocomposite materials [1–10]. LDH is available as both naturally occurring minerals and synthetic materials. The general composition of these intercalation materials can be represented as $[M^{2+}_{1-x}\ M^{3+}_x(OH)_2][(A^{n-})_{x/n}\cdot yH_2O]$, where M^{2+} and M^{3+} represent metallic cations such as Mg^{2+}, Ca^{2+}, Cu^{2+}, Mn^{2+}, Ni^{2+}, Zn^{2+}, and Al^{3+}, Cr^{3+}, Fe^{3+}, Mn^{3+}, Co^{3+}, respectively. A^{n-} is an anion of charge n such as Cl^-, CO_3^{2-}, NO_3^-, SO_4^{2-}, and organic anions. x value is equal to the molar ratio of $M^{3+}/(M^{2+}+M^{3+})$. The crystal structure consists of positively charged brucite-like octahedral hydroxide basal layers, which are electrically neutralized by the interlayer anions and water molecules occupying interlayer spaces [11,12].

Recently, the use of LDH as host material for the synthesis of organic–inorganic host–guest supramolecular structure has received great interest. The intercalation of organic compounds into LDH has been investigated from a wide range of scientific and practical interests, especially because of the nanostructures of the resulting intercalation compounds [13–16]. The intercalation of organic anions into LDH has been accomplished by the following methods: (I) an ion-exchange reaction with LDH containing monovalent anions such as chloride or nitrate [17–19], (II) a rehydration reaction of the calcined $M^{2+}-M^{3+}$ oxide precursor in the presence of an organic anions [18,20,21], (III) a coprecipitation reaction in which the LDH sheet is grown in the presence of the organic anion with exclusion of carbonate [18,22,23], and (IV) a thermal reaction, which mechanism is depend upon the removal of the interlayer carbonate anions with increasing the

*Corresponding author. Fax: +81-19-621-6331.
E-mail address: enarita@iwate-u.ac.jp (E. Narita).

0022-4596/03/$ - see front matter
doi:10.1016/S0022-4596(03)00234-2

temperature under above melting point of organic anions [24,25]. One of the most interesting features of the LDH is that the $M^{2+}-M^{3+}$ oxide precursor, which is produced by the thermal decomposition of the $CO_3/M^{2+}-M^{3+}$ LDH, can hydrate and take up a variety of organic anions from aqueous solutions, thereby reconstructing the original LDH structure. So far, many studies have been carried out on the intercalation of organic anions in the interlayer space of the LDH by this "calcination–rehydration reaction". Since the priority of anion uptake by the $M^{2+}-M^{3+}$ oxide precursor increases with increasing the electric charge of anion and with decreasing the anion size. The anion uptake behavior is believed to be governed mainly by the electrostatic interaction between LDH basal layer and interlayer anions.

On the other hand, the simplest sugars, monosaccharides, are the compounds with the general formula $(CH_2O)_n$, where n is an integer between 3 and 7. In nucleotides, one of several different nitrogen-containing ring compounds is linked to a five-carbon sugar (either ribose or 2-deoxyribose) with phosphate group. From the viewpoint of materials chemistry, sugar is a very interesting material due to the large number of structures of sugar and subsequent polymeric materials. It is, therefore, envisaged that new hybrid materials, the sugar/LDH composites, will be receiving much attention in future. H. Zhao and G.F. Vance reported the intercalation of carboxymethyl-β-cyclodextrin into the Mg–Al LDH [6,26]. They hypothesized that carboxymethyl-β-cyclodextrin (sodium salt) molecules would be sorbed into the interlayer of LDH because carboxymethyl-β-cyclodextrin could easily disassociate into negatively charged species. Moreover, the intercalation of biomolecule into LDH such as nucleotide, deoxyribonucleic acid, amino acid, and polypeptide has been investigated in order to prepare the biomolecule/LDH nanocomposite materials [19,23,27–29]. However, we know of no report concerning the intercalation of pure sugar possessing non-ionized structure into LDH.

In this study, we describe the synthesis and characterization of several new sugar/LDH nanocomposite derived by the "calcination–rehydration reaction" method using the CO_3/Mg–Al or Zn–Al LDH and pentoses (ribose and 2-deoxyribose).

2. Experimental

2.1. Materials

All reagents were of analytical grade and used without further purification. Ribose and 2-deoxyribose were purchased from Wako Pure Chemical Inc. (Japan).

2.2. Synthesis of Co_3/LDH

The CO_3/Mg–Al LDH was prepared following the standard coprecipitation described by Miyata [30]. In a typical synthesis, a mixed solution of 1 M $MgCl_2$ and 1 M $AlCl_3$ was slowly added to 1 M Na_2CO_3 solution at 298 K with vigorous stirring. The pH of the reaction mixture was maintained at pH 9–10 by the continuous addition of 2 M NaOH. The precipitate obtained was washed with water and added to 350 cm^3 of 1 M Na_2CO_3 solution. The resulting gel was aged with boiling for 5 h. A white solid product was subsequently isolated by centrifugation, washed with water and dried in a vacuum oven at 333 K for 24 h. All water was deionized and distilled before use. The CO_3/Zn–Al LDH was prepared in the same manner described above. The Mg/Al and Zn/Al molar ratio $[x = M^{3+}/(M^{2+} + M^{3+})]$ of the LDH was set up at 2/1 ($x = 0.33$) and 3/1 ($x = 0.25$) in this study.

2.3. Synthesis of sugar/LDH

The starting LDH was calcined at 773 K for 2 h to prepare the Mg–Al and Zn–Al oxide precursor. In the tests for the uptake of each sugar, 50 cm^3 of a sugar solution with various concentrations was placed in a 100 cm^3 Erlenmeyer flask together with 0.2 g of the M^{2+}–Al oxide precursor and shaken in a water-bath set at 298 K for 24–144 h. It was necessary to carry out the preparations under an inert N_2 atmosphere in order to exclude air, because the carbonated LDH forms preferentially in the presence of CO_2 gas. The suspension was filtered, washed several times with water to remove excess sugar, and dried under vacuum at 333 K for 24 h. The sugar concentration in the supernatant solution was measured using Shimadzu TOC-5000 total organic carbon (TOC) analyzer.

2.4. Deintercalation of sugar from sugar/LDH by ion exchange

Deintercalation experiment was conducted using the anion-exchange method using CO_3^{2-} ion. In the tests for the deintercalation of sugar, 50 cm^3 of Na_2CO_3 or $NaHCO_3$ solutions with various concentrations was placed in a 100 cm^3 Erlenmeyer flask together with 0.4 g of the sugar/LDH composite powder and was shaken in a water-bath set at 298 K for 24 h. The suspension was filtered, washed several times with water, and dried under vacuum at 333 K for 24 h. The supernatant solution was analyzed for the sugar concentration by TOC.

2.5. Characterization of solid products

Chemical analysis data for Al, Mg, and Zn were obtained using a Hitachi 180-80 atomic absorption spectrophotometer after dissolution of the solid products in 0.1 M HCl solution. XRD patterns were recorded on a Rigaku Rint 2200 powder X-ray diffractometer, using a CuKα ($\lambda = 0.15405$ nm) radiation with Ni filtered at 20 mA and 40 kV, 2θ angle ranged from 2–70°, and a scanning rate of 2°/min. FT-IR spectra were recorded on the sample pressed into KBr disc using a JASCO WS/IR 7300 FT-IR spectrophotometer. TG-DTA analyses were carried out using a Seiko TG/DTA 320 in the temperature 298–1173 K range with heating rate of 10 K/min in air flow. Solid-state ^{13}C-CP/MAS NMR spectroscopy was performed at 125.7 MHz with Varian Inova UNITY-500.

3. Results and discussion

3.1. Intercalation of sugar for LDH

The M^{2+}–Al oxides precursor used for the present intercalation experiments were obtained by heating of the synthetic, well-characterized LDH, $[Mg_{0.65}Al_{0.35}(OH)_2][(CO_3)_{0.18}\cdot 0.55H_2O]$, $[Mg_{0.75}Al_{0.25}(OH)_2][(CO_3)_{0.13}\cdot 0.62H_2O]$, $[Zn_{0.67}Al_{0.33}(OH)_2][(CO_3)_{0.17}\cdot 0.53H_2O]$, and $[Zn_{0.77}Al_{0.23}(OH)_2][(CO_3)_{0.12}\cdot 0.60H_2O]$ at 773 K for 2 h in a muffle furnace, respectively. The time dependence of the amount of ribose intercalated by the M^{2+}–Al oxide precursors is shown in Fig. 1. The amount of ribose intercalated by the Mg–Al oxide precursor increased continuously until the equilibrium was reached after about 120 h. All experiments were continued for 144 h to ensure that the equilibrium was attained. The chemical composition of the resulting ribose/LDH obtained at 120 h is shown in Table 1. The maximum intercalated amounts of ribose by the Mg–Al oxide precursor ($x = 0.25$) and ($x = 0.33$) are 542 and 435 mmol/mol-Al (3.15 ($x = 0.25$) and 3.45 ($x = 0.33$) mmol/g-oxide), respectively, while these values by the Zn–Al oxide precursor ($x = 0.25$) and ($x = 0.33$) are 32.7 and 46.3 mmol/mol-Al (0.12 ($x = 0.25$) and 0.25 ($x = 0.33$) mmol/g-oxide). Namely, the uptake ability of the Mg–Al oxide precursor ($x = 0.25$) is about 20 times that of the Zn–Al oxide precursor ($x = 0.25$). In the case of the Zn–Al oxide precursor, the rehydration reaction was thought to be inhibited by the formation of the ribose/Zn complex on the surface of the oxide precursor, which caused the extremely small amount of ribose intercalated was thought to be decreased. Therefore, we chose the Mg–Al oxide precursor rather than the Zn–Al oxide precursor as the host in further studies. Fig. 1 also indicates that the Mg–Al oxide precursor ($x = 0.25$) has slightly higher uptake ability than the Mg–Al oxide precursor ($x = 0.33$). It is suspected that the OH^- having a small ionic size is preferentially intercalated into the Mg–Al LDH interlayer ($x = 0.33$) over ribose, because the hydroxide basal layer has a high charge density. The equilibrium pH values of the Mg–Al LDH ($x = 0.33$) and ($x = 0.25$) were found to be 8.1 and 8.7 at 144 h, respectively. This result supports that the Mg–Al LDH ($x = 0.33$) would contain a higher amount of OH^- into the interlayer compared to the Mg–Al LDH ($x = 0.25$).

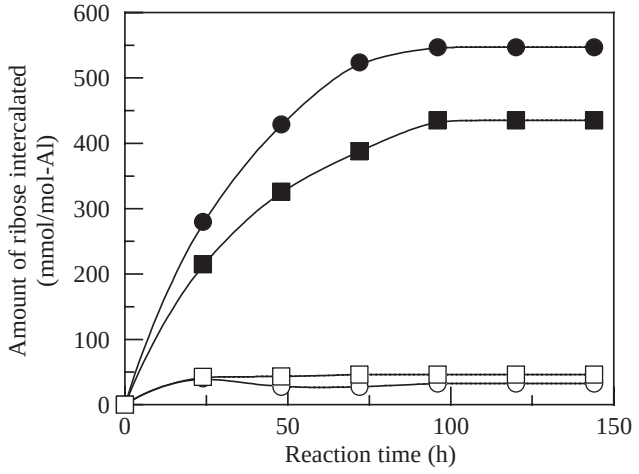

Fig. 1. Time dependence of amount of ribose intercalated by Mg–Al and Zn–Al oxide precursors at 298 K. Initial concentration of ribose is 50 mM. (●) Mg–Al oxide $x = 0.25$, (■) Mg–Al oxide $x = 0.33$, (○) Zn–Al oxide $x = 0.25$, and (□) Zn–Al oxide $x = 0.33$.

Table 1
Chemical composition of ribose/LDH

M^{2+}–Al	Molar ratio	Chemical composition
Mg–Al	2/1	$[Mg_{0.66}Al_{0.33}(OH)_2]$ $[ribose_{0.15}(CO_3)_{0.10}OH_{0.13}\cdot 0.49H_2O]$
Mg–Al	3/1	$[Mg_{0.75}Al_{0.25}(OH)_2]$ $[ribose_{0.14}(CO_3)_{0.09}OH_{0.07}\cdot 0.45H_2O]$
Zn–Al	2/1	$[Zn_{0.66}Al_{0.33}(OH)_2]$ $[ribose_{0.02}(CO_3)_{0.16}OH_{0.01}\cdot 0.60H_2O]$
Zn–Al	3/1	$[Zn_{0.75}Al_{0.25}(OH)_2]$ $[ribose_{0.01}(CO_3)_{0.12}OH_{0.01}\cdot 0.59H_2O]$

The XRD patterns of the synthetic pristine LDH, M^{2+}–Al oxide precursor and resulting solid products are shown in Fig. 2. The CO_3/Mg–Al LDH and Zn–Al LDH show the (003) spacing of 0.77 nm and 0.76 nm in Fig. 2a and d, and these values are in good agreement with those of the other CO_3/LDHs, respectively. The layered structure was destroyed by heating of the LDH at 773 K for 2 h, which can be seen by the disappearance of (003) and (006) reflections in the XRD pattern of the M^{2+}–Al oxide LDH in Fig. 2b and e. The Mg–Al LDH containing ribose showed expanded structures

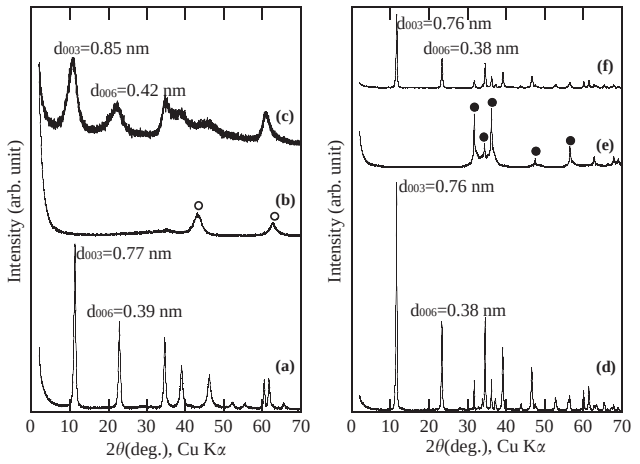

Fig. 2. Powder XRD patterns of: (a) CO_3/Mg–Al LDH, (b) Mg–Al oxide, (c) ribose/Mg–Al LDH, (d) CO_3/Zn–Al LDH, (e) Zn–Al oxide, and (f) ribose/Zn–Al LDH.

with a broad (003) spacing of 0.85 nm in Fig. 2c. Molecular size of ribose is calculated as 0.44 nm in length, 0.43 nm in width, and 0.36 nm in thickness. This expanded interlayer separation is consisted with the intercalation of the ribose in the interlayer spaces of the LDH. As a thickness of the LDH host layer is 0.48 nm, the interlayer distance of the ribose/Mg–Al LDH is calculated as 0.37 nm, and this value suggests that ribose is oriented horizontally in the interlayer space. However, the broadness of these peaks indicates that the resulting nanocomposites does not constitute an organized stacking arrangement. Hydroxyl and carbonate ions were also cointercalated within interlayer space, consistent with a broad XRD peak at 0.85 nm, which was attributed to disordered layers of OH^- within the ribose/Mg–Al LDH nanocomposites. The molar ratio of Mg^{2+}/Al^{3+} did not have an influence on the XRD patterns of the ribose/Mg–Al LDH nanocomposites. The XRD patterns for the ribose/Zn–Al LDH exhibit a relatively sharp set of (00*l*) reflections, indicating highly organized stacking arrangements. Nevertheless, these basal spacing is the same as that of the CO_3/Zn–Al LDH (Fig. 2f). Since these nanocomposites contained small amounts of ribose in the interlayer space, the high crystallinity is explained by the priority presence of OH^- in spite of ribose. It seems that ribose is hardly intercalated into the Zn–Al LDH interlayer space.

The FT-IR spectra of the Mg–Al LDH ($x = 0.25$), Zn–Al LDH ($x = 0.25$), and related nanocomposites are shown in Fig. 3. The strong peak at 1375 cm^{-1} and bread peak at 1560 cm^{-1} are attributed to the stretching mode of CO_3^{2-} (Fig. 3a and c). The peaks at 660 and 428 cm^{-1} are associated with *M*–O and O–*M*–O stretching modes in the LDH sheets. The ribose/Mg–Al LDH nanocomposite exhibits the FT-IR peaks characteristic of both the ribose and LDH sheets. The

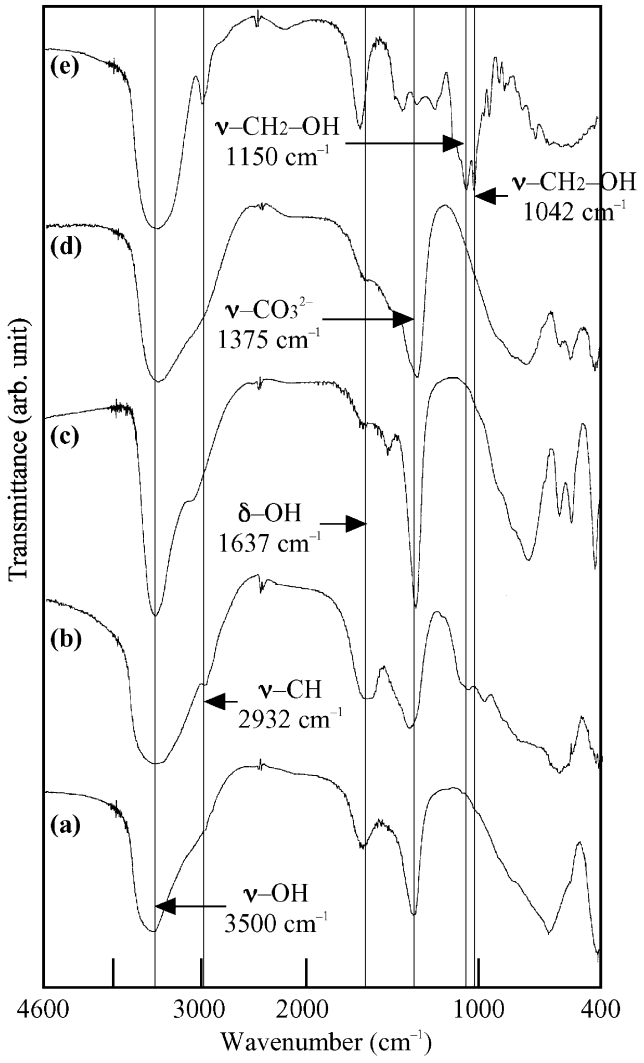

Fig. 3. FT-IR spectra of: (a) CO_3/Mg–Al LDH, (b) ribose/Mg–Al LDH, (c) CO_3/Zn–Al LDH, (d) ribose/Zn–Al LDH, and (e) ribose.

FT-IR spectrum contains peaks at 1042 cm^{-1} and 2932 cm^{-1} which are characteristic of C–O stretching and C–H stretching in ribose (Fig. 3b,d and e). The ribose/Zn–Al LDH nanocomposite exhibits the FT-IR peaks characteristic of only the LDH sheets. This result supported the small amount of ribose in the Zn–Al LDH ($x = 0.25$), only 0.12 mmol/g-oxide.

The ^{13}C-CP/MAS NMR spectra of the ribose/Mg–Al LDH ($x = 0.25$) nanocomposite and ribose as a reference are shown in Fig. 4. Ribose has two conformations, furanose and pyranose. The resonances attributed to ribose at 56.1 ppm (C-5), 67.9–72.8 ppm (C-2–4), 92.7 ppm (C-1), and 95.1 ppm (C-1) are observed in Fig. 4b, supporting that the conformation of ribose is pyranose. In the case of the ribose/Mg–Al LDH nanocomposite, the resonances attributed to the intercalated ribose at 64.3 ppm (C-5), 74.9 ppm (C-2–4), 84.5 ppm (C-4), and 99.9 ppm (C-1) are observed in

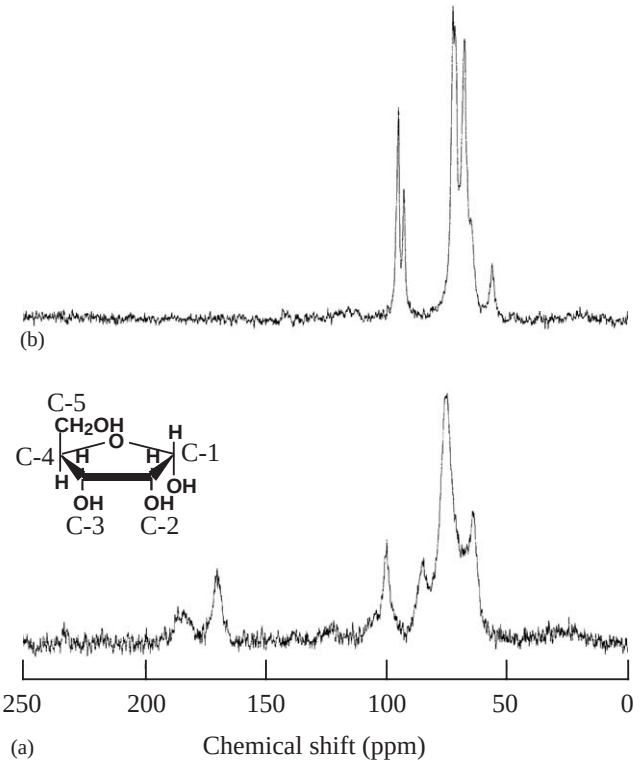

Fig. 4. ^{13}C-CP/MAS NMR spectra of: (a) ribose/Mg–Al LDH and (b) ribose.

Fig. 4a. This result supported that the intercalated ribose is furanose. Moreover, the resonance of the cointercalated CO_3^{2-} is also observed at 170.2 ppm. This result indicates that the conformation of almost ribose in the LDH interlayer space was transformed from pyranose into furanose.

The results from TG analysis for the CO_3/Mg–Al LDH ($x = 0.25$), the ribose/Mg–Al LDH ($x = 0.25$) nanocomposite and ribose are shown in Fig. 5. The CO_3/Mg–Al LDH shows weight loss in two steps. The first, corresponding to ca. 15% loss between 323 and 483 K, was attributed to elimination of both surface adsorbed water and interlayer water molecules. The second, ca. 30% between from 573 and 723 K, was derived from both CO_2 losses by the decomposition of carbonate and water loss by dehydroxylation of the brucite layers. The total loss was ca. 45% of the initial sample weight. In the case of the ribose/Mg–Al LDH nanocomposite, the total weight loss was 52%. The gentle weight loss due to the removal of the adsorbed water, interlayer water, and dehydroxylation of the brucite layer were observed in the temperature region 298–600 K. The rapid weight loss was subsequently observed by the combustion of the intercalated ribose in the temperature region 600–700 K.

To confirm this interesting driving force in interaction with the non-ionized organic guest into the Mg–Al

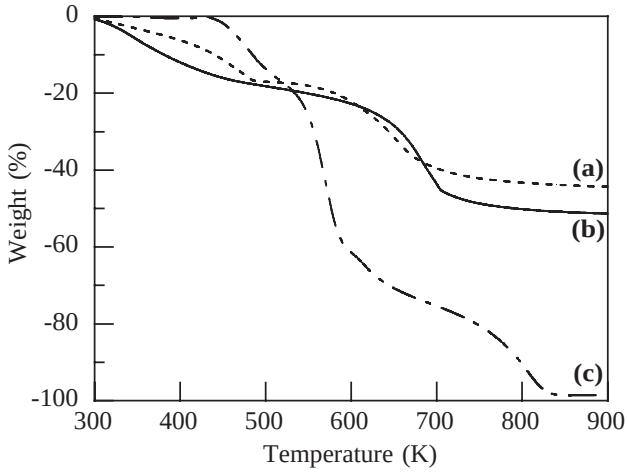

Fig. 5. TG curves of: (a) CO_3/Mg–Al LDH, (b) ribose/Mg–Al LDH, and (c) ribose.

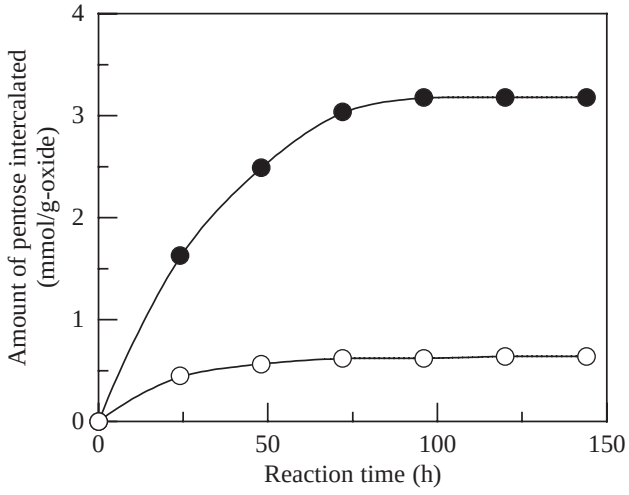

Fig. 6. Time dependence of amount of pentoses intercalated by Mg–Al oxide ($x = 0.25$) at 298 K. Initial concentration of pentoses is 50 mM. (●) ribose and (○) 2-deoxyribose.

LDH, the Mg–Al LDH ($x = 0.25$) was evaluated for its ability to intercalate other guests, such as 2-deoxyribose which is only substituted by hydrogen at C-2 position for ribose. The amount of 2-deoxyribose intercalated by the Mg–Al oxide precursor is shown in Fig. 6. The equilibrium pH value became 10.9 from the initial pH value 4.9 after 144 h. The maximum uptake amount of 2-deoxyribose by the Mg–Al oxide precursor ($x = 0.25$) was 46.3 mmol/mol-Al or 0.214 mmol/g-oxide at 72 h. In contrast, the maximum value for ribose mentioned previously was 542 mmol/mol-Al or 3.15 mmol/g-oxide at 120 h, indicating about 5 times that for 2-deoxyribose. The amount (X/M) of ribose and 2-deoxyribose intercalated by the Mg–Al oxide precursor ($x = 0.25$) was determined at various initial concentrations of the

non-anionic guests, and results are shown in Fig. 7. The amount of pentoses intercalated was found to increase slightly with the increase in the equilibrium concentration of the solutions. In all cases, the Freundlich isotherm, $\log(X/M) = 1/n(\log C) + \log k$, is applicable. X (mg) is the amount of adsorbed guests, M (g) is the amount of the LDH, C (mmol/L) is equilibrium concentration of guests, k and n are constants. The k and n values were obtained from the intercept and slope of the isotherms, respectively. The absorbability for ribose ($k = 1.1$ mmol/g-oxide) was quite higher than that for 2-deoxyribose ($k = 0.052$ mol/g-oxide), indicating that the Mg–Al LDH has a stronger affinity for ribose than 2-deoxyribose.

The Mg–Al LDH ($x = 0.25$) containing 2-deoxyribose showed the layer structure with (003) and (006) diffraction peaks at 0.77 and 0.39 nm, which are quite similar to those of the CO_3/Mg–Al LDH. This implies that the Mg–Al precursor reconstructed the original hydrotalcite-like structure with incorporating the water molecules, a slight amount of 2-deoxyribose, and OH^- which being preferentially incorporated over 2-deoxyribose.

The schematic model of the intercalation of ribose in the Mg–Al LDH by the calcination–rehydration reaction is shown in Fig. 8. The XRD pattern of the ribose/Mg–Al LDH ($x = 0.25$) nanocomposite indicates that the molecular plane of ribose is horizontally oriented to the hydroxide layers, but that of the 2-deoxyribose/LDH nanocomposites showed the same structure of the CO_3/Mg–Al LDH (Fig. 2a). It was well known that the molecular configuration, conformation, and size of 2-deoxyribose are similar to that of ribose, except ribose is substituted by a hydroxyl group at C-2 position. In the case of ribose, it seems that the presence of the hydroxyl group favors by the intercalation hydrogen bonding with the hydroxide basal layer, possibly resulting in the formation of a ribose monolayer arrangement. These results suggest that the Mg–Al oxide precursor induces the selective intercalation of non-ionized organic guests. Therefore, we would like to propose here that the hydrogen bond participates in the intercalation of non-ionized organic guests by the Mg–Al oxides precursor under an inert N_2 atmosphere.

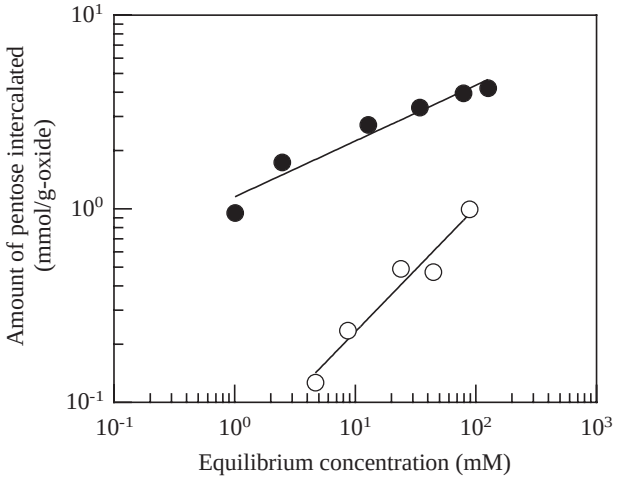

Fig. 7. Intercalation isotherms of: (●) ribose and (○) 2-deoxyribose by Mg–Al oxide at 298 K after 120 h.

3.2. Deintercalation of ribose from ribose/Mg–Al LDH

The results of the deintercalation experiments confirmed that more than 40% of ribose in the Mg–Al LDH ($x = 0.25$) was deintercalated by shaking with 250 mM Na_2CO_3 or $NaHCO_3$ solution for 24 h (data not shown). The ribose in the interlayer space of the resulting LDH has easily deintercalated by the ion exchange with carbonate ions. The XRD pattern of the deintercalated product also showed that the original CO_3/Mg–Al LDH was regenerated with $d_{003} = 0.77$ nm. It seems that ribose molecules are intercalated into the interlayer space, not adsorbed on surface. These results show that the cycle system of intercalation and deintercalation for ribose into LDH would be widely applicable to several cases such as synthesis of new hybrid organic–inorganic nanocomposites.

4. Conclusion

This investigation has led to a new finding for the intercalation of the non-ionized biomolecules, pentoses, into the interlayer LDH. Some of the important findings

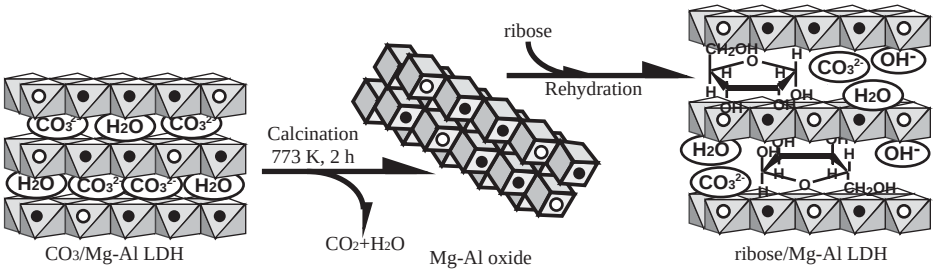

Fig. 8. Schematic representation of ribose oriented in interlayer space of Mg–Al LDH.

of this study can be summarized as follows. (I) The non-ionized sugar/LDH nanocomposite, containing ribose, can be prepared by the calcination–rehydration reaction using Mg–Al LDH. The maximum amount of ribose intercalated by the Mg–Al oxide precursor was approximately 20 times that by the Zn–Al oxide precursor. (II) With regarded to the kind of pentose for the Mg–Al LDH, the maximum intercalated amount of ribose molecules was approximately 5 times that of 2-deoxyribose. The presence of the OH group in pentose favors the intercalation driving by the hydrogen bonding with the hydroxide basal layer. (III) The Mg–Al LDH containing ribose showed the expanded LDH structures with a broad (003) spacing of 0.85 nm. The interlayer distance of the ribose/Mg–Al LDH nanocomposite is 0.37 nm, and this value suggests that ribose is oriented horizontally in the interlayer. (IV) The interesting feature of this preparative method is that a wide variety of non-ionized organic guests can be intercalated between the hydroxide sheets. This synthetic procedure can be applicable to the preparation of LDH containing non-ionized organic guests, which are difficult to obtain in any other ways. (V) New sugar/clay nanocomposites, being both environmentally and economically, may receive considerable attention in the future and might have uses as new type clay with bioactive and biodegradative properties.

Acknowledgments

The authors are grateful to Dr. H. Nakayama (Kobe Pharmaceutical University) for the measurements of ^{13}C-CP/MAS NMR spectra and his helpful advice. Thanks are also given to Mr. S. Takahashi (technical officer, Iwate University).

References

[1] F. Cavani, F. Tirifiro, A. Vaccari, Catal. Today 11 (1991) 173.
[2] B. Sels, D. De Vos, M. Buntinx, F. Pierard, A.K. Mesmaeker, P. Jacobs, Nature 400 (1999) 855.
[3] H. Sakaebe, H. Uchino, M. Azuma, M. Shikano, S. Higuchi, Solid State Ionics 113–115 (1998) 35.
[4] J. Qiu, G. Villemure, J. Electroanal. Chem. 428 (1997) 165.
[5] T. Kuwahara, H. Tagaya, J. Kadokawa, K. Chiba, J. Mater. Synth. Proc. 4 (1996) 69.
[6] H. Zhao, G.F. Vanece, Clays Clay Miner. 46 (1998) 712.
[7] Y. Seida, Y. Nakano, Water Res. 36 (2002) 1306.
[8] S.P. Newman, W. Jones, N. J. Chem. 22 (1998) 105.
[9] F. Leroux, J.-P. Besse, Chem. Mater. 13 (2001) 3507.
[10] S. Aisawa, S. Takahashi, W. Ogasawara, Y. Umetsu, E. Narita, J. Solid State Chem. 162 (2001) 52.
[11] L. Ingram, H.F.W. Taylor, Mineral Mag. 36 (1967) 465.
[12] R. Allmann, Acta Crystallogr. Sect. B 24 (1968) 972.
[13] J.-H. Choy, S.-Y. Kwak, J.-S. Park, Y.-J. Jeong, J. Mater. Chem. 11 (2001) 1671.
[14] F. Leroux, M.A.-Pagano, M. Intissar, S. Chauvière, C. Forano, J.-P. Besse, J. Mater. Chem. 11 (2001) 105.
[15] T. Hibino, W. Jones, J. Mater. Chem. 11 (2001) 1321.
[16] N. Iyi, K. Kurashima, T. Fujita, Chem. Mater. 14 (2002) 583.
[17] M. Meyn, K. Beneke, G. Lagaly, Inorg. Chem. 29 (1990) 5201.
[18] M. Kaneyoshi, W. Jones, J. Mater. Chem. 9 (1999) 805.
[19] Á. Fudala, I. Pálinkó, I. Kiricsi, Inorg. Chem. 38 (1999) 4653.
[20] T. Sato, K. Kato, T. Yoshioka, A. Okuwaki, J. Chem. Technol. Biotechnol. 55 (1992) 385.
[21] H. Tagaya, S. Sato, H. Morioka, J. Kadokawa, M. Karasu, K. Chiba, Chem. Mater. 5 (1993) 1431.
[22] S. Aisawa, S. Takahashi, W. Ogasawara, Y. Umetsu, E. Narita, Clay Sci. 11 (2000) 317.
[23] S. Aisawa, H. Hirahara, H. Uchiyama, S. Takahashi, E. Narita, J. Solid State Chem. 167 (2002) 152.
[24] S. Carlino, M.J. Hudson, J. Mater. Chem. 4 (1994) 99.
[25] S. Carlino, M.J. Hudson, J. Mater. Chem. 5 (1995) 1433.
[26] H. Zhao, G.F. Vance, J. Chem. Soc. Dalton Trans. (1997) 1961.
[27] J.-H. Choy, S.-Y. Kwak, J.-S. Park, Y.-J. Jeong, J. Portier, J. Am. Chem. Soc. 121 (1999) 1399.
[28] J.-H. Choy, S.-Y. Kwak, Y.-J. Jeong, J.-S. Park, Angew. Chem. Int. Ed. 39 (2000) 4042.
[29] N.T. Whilton, P.J. Vickers, S. Mann, J. Mater. Chem. 7 (1997) 1623.
[30] S. Miyata, Clays Clay Miner. 23 (1975) 369.